Parasitology International 71 (2019) 18–26

Contents lists available at ScienceDirect

Parasitology International

journal homepage: www.elsevier.com/locate/parint

Impact of autophagic regulation on splenic red pulp macrophages during cerebral malarial infection

Anirban Sengupta[a], Samrat Sarkar[a], Tarun Keswani[b], Saikat Mukherjee[a], Soubhik Ghosh[a], Arindam Bhattacharyya[a,*]

[a] Immunology Laboratory, Department of Zoology, University of Calcutta, 35, Ballygunge Circular Road, Kolkata 700019, India
[b] Basic and Clinical Immunology of Parasitic Diseases, Univ. Lille, CNRS, Inserm, CHU Lille, Institut Pasteur de Lille, U1019, UMR 8204, CIIL - Centre of Infection and Immunity Lille, F-59000 Lille, 1 rue du Professeur Calmette, 59019 Lille, France

ARTICLE INFO

Keywords:
Autophagic flux
Macroautophagy
Plasmodium bergheei ANKA
Chemokine regulation
Pathogen processing
Pathogenic degradation
T cell infiltration

ABSTRACT

Splenic red pulp macrophages play a critical role infiltration of infected RBC and elimination of pathogens during malarial infection. However, the efficiency of pathogenic processing and the intricate pathway followed by them to boost the downstream immune response has not been studied in details. We checked the status of autophagic regulation within the cells both before and after the infection and also modulated the autophagic flux with either its inducer or inhibitor. We found that the upregulation of autophagic gene and the corresponding pathway is correlated with better parasite clearance and survivability, with an enhanced downstream immune response. It also increases their phagocytic potential with better Lysosomal associated protein I and II synthesis. The autophagolysosome formation increases as well, and more vacuole bound LC3B protein are detected. Chemokine synthesized from Red Pulp macrophage helps in mediating the induction for recruiting neutrophil and CD4 + T cells to the splenic red pulp region. The skewing of M1 macrophage polarity is observed post autophagic induction with a better costimulatory molecule like CD80, CD86 expression and antigen presenting molecule MHC I, MHC II is observed. This study shows the possibility of an alternative or adjuvant therapy regimen for the malarial patient by inducing the autophagic pathway that targets the red pulp macrophages. This might be helpful for better pathogen degradation and processing. The subsequent clearance of parasite will result in a better outcome for the patients.

1. Introduction

Mouse model of Experimental Cerebral Malaria (ECM) recapitulates most of its characteristics with its human counterpart, with about 100% lethality within 6–14 days post-infection [1,2]. *Plasmodium bergheei* ANKA (PbA) is the mouse homolog for *Plasmodium falciparum*. It kills millions of people worldwide every year [2]. The disease is accompanied by neurological damage, ataxia, paralysis, convulsion, and coma [1,2]. ECM initiates after the processing and presenting of infected RBC (iRBC) antigens by splenic antigen presenting cells like dendritic cells and macrophages. These antigens, in turn, primes naïve CD4T and CD8T cells of the spleen. Inflammatory cytokine secretion and the subsequent activation of brain endothelium for antigen presentation and chemokine secretion attract the primed effector CD8T cell [4]. This T cell population got engaged with the MHC I peptide complex on brain endothelium resulting in the release of perforin, granzymes, chemokines. These attract Natural Killer (NK) cells and macrophages to the brain [5,6]. Together these immune cells breach the Blood-Brain Barrier (BBB) by perturbing the endothelium, causing the full-blown cerebral malarial pathogenesis [3].

Blood-borne pathogen clearance is a hallmark feature of the lymphoid organ spleen. Splenic Red Pulp is bathed in the slow-paced bloodstream of venous cords and sinuses, which in turn facilitates the filtration of the blood and in the elimination of damaged or infected Red Blood Cells (RBC) [7]. Apart from the phagocytosis and pathogenic clearance by Red Pulp Macrophages (RPM) they also play a crucial role in immune system activation. Splenomegaly is one of the most prominent symptoms of Plasmodium infection [8].

Macroautophagy (hereafter autophagy) plays a crucial role in the degradation and processing of the engulfed pathogens within the macrophage. [9]. Literature report suggests that the breakdown of pathogens within the cells require a proper and complete autophagic flux. Autophagic flux blockage causes poor disease outcome in different infectious diseases [10]. No previous study looked into the effect of the

* Corresponding author.
E-mail address: arindam19@gmail.com (A. Bhattacharyya).

https://doi.org/10.1016/j.parint.2019.03.008
Received 5 November 2018; Received in revised form 8 March 2019; Accepted 8 March 2019
Available online 11 March 2019

autophagic pathway within the splenic immune cells during malarial infection.

Autophagolysosome formation, autophagic pathway gene expression, protein activity, autophagic marker protein LC3B accumulation in the vacuoles are few of the many essential steps of the pathway reported assessing a proper autophagic flux progression [11]. The adhesion property of the RPM towards the control or infected RBC, along with their phagocytic property is essential for the engulfment of the pathogen to undergo a pathogenic degradation process [12].

We previously reported splenic cell apoptosis during the Plasmodium infection [13]. Both apoptosis and Plasmodium infection results in the upregulation of endogenous HMGB1 serum level, which plays a direct role in autophagic induction in many other scenarios [14]. RPMs are efficient phagocytes and produce proinflammatory cytokines like type I IFNs and TNFa [15]. Interestingly, autophagy-mediated degradation of the NF-kB inhibitor molecule A20 [16] releases CXCL1 and CXCL2 resulting in the neutrophil recruitment in spleen by RPM [17].

RPM produces chemokines that directly binds with the CXCR3 and CXCR5 found in upregulated condition within the CD4 + T cells and thus recruit helper T cells [17]. The variable cytokine milieu in the red pulp microenvironment during the acute infection phase dictates RPM function [18]. Enhanced iron accumulation capacity by classic M1 MΦs positively influences the maintenance of these cells in a proinflammatory state [19]. Low iron level released from the hemozoin breakdown during the malarial infection may skew the macrophage to alternate activation pathway or M2 macrophage. They can produce anti-inflammatory cytokines like Tgf-b, IL10 and generate T regulatory cells [20].

Mammalian target of Rapamycin (mTOR) acts as a central regulator for both innate and adaptive immune responses by determining T cell fate post-differentiation, T cell activation and clonal expansion [21,22]. Rapamycin previously reported having a beneficial host immune response in ECM pathogenesis with a significant increase in survivability potential [3]. Blocking of BBB breakdown, brain hemorrhage, the influx of CD4 and CD8 T cells to the brain and accumulation of iRBC in the brain are few established mechanisms of rapamycin-mediated host protection against ECM [3].

Rapamycin is reported to possess microbicidal property against Plasmodium parasites [23]. It can interact with *Plasmodium falciparum* FK506 binding protein *Pf*FKBP35 and can inhibit parasite growth [24]. Dihydroartemisinin, an active metabolite in all artemisinin-derived antimalarials, also reported inhibiting mTOR in cells [25] and mice [26]. Dietary restrictions reduce parasite accumulation in peripheral tissues including the brain and increase clearance in the spleen by activating nutrient-deprived autophagy via the mTOR pathway [27]. Another mTOR inhibitor, torin2 also reported having a beneficial role in pathogen clearance [28]. However, the identification of putative protein binding partners for torin2 within the plasmodium metabolic pathway suggests that its beneficial role might not be mTOR pathway mediated [29]. On the other hand, rapamycin is an FDA approved the drug and is safe on the human. Hence, we choose rapamycin as our drug of interest to modulate the mTOR pathway and thus acts as an autophagic inducer.

Ammonium Chloride is used as a lysosomotropic agent which accumulates in lysosomes. It then increases the low pH of lysosome which results in blocking of autophagic flux [30]. The compound is widely used as an autophagy inhibitor for decades [31,32], and is also used in our study for the same.

We hereby interested in studying the influence of autophagic induction have on splenic RPM during ECM. We dissected out multilayered steps of the autophagic pathway and analyzed their status in correlation with the parasite load and clearance along with the survivability of the model organism. During the process, we checked various chemokine levels synthesized by RPM and its impact on the recruitment of other immune cells to the splenic red pulp region. Overall, we provide a comprehensive report of the autophagic flux and its importance and consequence of the modulation of the same in malarial infection within splenic RPM.

2. Material methods

2.1. Materials

The materials used for this study including the antibodies, primers, kits, dyes and other reagents are provided in the supplementary material under 'Materials' section.

2.1.1. Malaria mice model development

Male Swiss albino mice (~25 g each; aged 6–8 weeks) were housed five per cages and were provided with rodent chow (National Institute of Nutrition, India) and filtered water ad libitum. Animal experiments were carried out as per the guidelines. of the Committee for the purpose of Control and Supervision of Experimental Animals (CPCSEA), Government of India (Registration No: 885/ac/05/CPCSEA) and as approved by the Institutional Animal Ethics Committee (IAEC), University of Calcutta, and confirms with the Guide for the Care and Use of Laboratory Animals published by the US National Institutes of Health. *P. berghei ANKA* parasite strain was obtained from the National Institute Malaria Research Center, New Delhi. Liquid N_2 stored parasitized mouse red blood cells (pRBC) were injected (1×10^6 pRBC, in 100 µl PBS) into mice of the same background. After amplification, mice were infected with PbA (1×10^6 pRBC) in 100 µl PBS by intraperitoneal injection. Control mice were injected with an equal number of uninfected erythrocytes.

Daily parasitemia monitoring in all experimental groups was done by Giemsa-stained thin blood smears made from tail snips. The percentage of parasitemia was calculated as follows: parasitemia (%) = [(number of infected erythrocytes)/(total number of erythrocytes counted)]. Survivability and parasitemia of mice were also observed daily.

2.1.2. In vivo rapamycin and ammonium chloride dose and treatment groups

Rapamycin treatment was provided at 15 mg/kg body weight intraperitoneally, and ammonium chloride at 50 mg/kg orally once every day starting from one-day prior infection dose until the 8th-day post infection. On the day 8 post-infection, they are sacrificed, spleen harvested and RPM isolated. All experiments like RNA isolation for gene expression, phagocytosis assay, adhesion assay, autophagosome formation assay are performed on the isolated RPM from the control and three treatment groups i.e. only PBA infected, PBA + Autophagy inducer treated, PBA + Autophagy Inhibitor treated. Set of five mice (n = 5) are used in each of the aforesaid four groups for each experiment replicate. Total of four rounds of replicates per experiment are performed. Hence 5 mice/set X 4 treatment groups X 4 replicates = 80 mice are used for the whole study.

2.1.3. Flow cytometry and sorting

Euthanized mice are sacrificed on 8th day post infection and spleens are harvested out. The single cell suspension prepared from the spleen by mechanical tapping and passing through the cell strainers. The cells were centrifuged at 1000 rpm for 10 min at 4 °C and supernatant discarded. The pellet is then resuspended in 2 ml RBC Lysis Buffer and incubated for 5 min at room temperature. At the end of 5 min, the cells are centrifuged at 1000 rpm for 10 min at 4 °C and pellet was resuspended in Phosphate buffer saline (PBS) for washing. This step is repeated twice, and then the cells are resuspended in cell staining buffer containing 2% FBS in PBS.

The cells were first blocked with anti-CD16/CD32 and washed twice with PBS. They are then incubated with the required antibodies according to the experiment following manufacture's protocol for

antibody dilution, incubation duration, etc. In the cases for detection of intracellular protein markers, the cells are permeabilized with phosphate buffer saline (PBS) solution containing 0.1% Triton X-100 for 45 min and washed before the antibody incubation. The live population is determined by gating on viable forward versus side scatter gates. Isotype-matched antibodies were used as staining controls. The data are compensated for the fluorescence spill over to other filters. Labeled cells were acquired using a BD C6 Accuri Machine and analyzed by the Accuri C6 software.

F4/80 + (APC)CD68 + (PE) RPM subsets are sorted by BD FACS Verse III. Cell population was first gated out by forward and side scatter profile. The RPM are sorted only from live and single cell population as observed from the scatter profile. The sorted cells are collected in serum rich culture media (10% Fetal Bovine Serum containing DMEM) before further processing.

The antibody details are provided in the supplementary 'Materials' section.

2.1.4. Real-time Gene expression study

Total RNA extraction from the isolated RPM of different treatment groups was performed using TriZol reagent (Bangalore Genei, India), reverse transcribed (MMLV High-Performance Reverse Transcriptase, Epicentre Biotechnologies) (Random hexamer – Promega # C1181). 50 ng of cDNA is used per reaction of the realtime PCR for 35 cycles of amplification with primers for specific genes (Supplementary Table no:1). GAPDH was used as a constitutive expression. Syber Green reagent (Thermo Fisher: 4309155) used for The Real-time gene expression study and data acquired in Applied Biosystem StepOne RealTime Machine and analyzed in Applied Biosystem software.

2.1.5. Enzo dye for autophagic detection

The autophagolysosome detection within the isolated RPM is performed according to the manufacturer's protocol (ENZ:-51031) and also as performed by other groups [33]. Briefly, the cells are put into the buffer provided in the kit and incubated with the cyto-id dye following the dilution and incubation time from the kit instruction manual. The probe is a cationic amphiphilic tracer (CAT) dye and has careful selection of titratable functional moieties which prevents its accumulation within lysosomes but enables labeling of autophagolysosome vacuoles with minimum or no staining of the lysosomes. The post-staining wash by using buffer provided exclude the free excess dye. This step is repeated thrice to ensure maximum clearance of non-specific binding. The cells are then suspended in the suspension buffer, and the flow cytometric reading was taken immediately to minimize the loss of signal due to bleaching. The change in the fluorescence intensity emitted by the dye from different treatment samples is recorded via the green filter in the flow cytometry machine (BD C6 Accuri) and analyzed by the BD Accuri C6 software.

2.1.6. Flowcellect autophagy detection

Isolated RPM are subjected to serial washing steps as prescribed in the Flowcellect Autophagy Detection kit (Millipore: FCCH100171) and followed the methods as mentioned before [34]. Incubation and washing with the kit provided buffers results in depletion of cytoplasmic free LC3B protein while retaining the autophagic vacuole bound LC3B. The samples are then incubated with the LC3B-FITC antibody provided in the kit according to specific dilution and duration. To reduce the background signal from the non-specific binding of the dye, the post-incubation washing step is repeated thrice. Finally, the cells are suspended in the ice cold cell staining buffer (2% FBS in PBS). Reading was taken immediately using the green filter of the flow cytometry machine. The fluorescence emitted is detected by flow cytometry (BD C6 Accuri) and analyzed by the same software provided with the instrument.

2.1.7. Phagocytosis assay

Fluorochrome tagged zymosan A granules (Sigma: Z4250) [35] are co-incubated with RPM in the cell culture medium (DMEM, 5% FBS) for 2 h at 37 °C, 5% CO_2 cell culture incubator. The concentration, proportion, and dilution of the granules are done according to datasheet provided. The post-incubation masking of fluorochrome signal from non-ingested granules by trypan blue solution was performed as per manufactures protocol. Washing was performed by PBS thrice; each round being followed by the centrifugation 2000 rpm for 10 min at 4 °C and supernatant was discarded. Final resuspension was done on cell staining buffer, and immediately fluorochrome signal is detected by the green filter of BD accuri C6 machine and analyzed by BD C6 software.

2.1.8. Adhesion assay

To have a quantitative measurement of the number of infected RBC (iRBC) adhered to the sorted RPM, the iRBC extracted by heart puncture of the mice on the day of sacrifice was first labeled with calcein AM (Sigma: 17783) [36]. The labeling was performed in a medium containing 1.93 M of the cell-permeable fluorescent indicator, for 15 min at 37 °C and 7.5% CO_2. The excess fluorescent dye was removed by washing the cells thrice with ice-cold PBS without Ca2/Mg2. Each washing step is followed by centrifugation at 2000 rpm for 10 min at 4 °C and supernatant was discarded. The calcein-AM labeled iRBC pellet resuspended and co-incubated with RPM in the cell culture medium (DMEM, 5% FBS) for 2 h at 37 °C, 5% CO_2 cell culture incubator. Post incubation washing was performed by PBS thrice, each round being followed by the centrifugation as stated above. Final resuspension was done on cell staining buffer after which the fluorescence signal is detected by green filter 1 in BD FACS Accuri C6 followed by required analysis.

2.2. Statistical analysis

Values between groups under different treatment condition were analyzed using ANOVA, and by Tukey test where applied. Data are expressed as mean ± SEM unless indicated otherwise. Statistical analyses were performed in GraphPad Prism, one-way analysis of variance (ANOVA) or Kaplan–Meier survival tests as indicated. Data were analyzed, and when appropriate, the significance of the differences between mean values was determined using Student's *t*-test. Significant differences were assessed by the Log-rank test. $p < .05$ were considered significant ($^{*}p < .05$, $^{**}p < .01$ and $^{***}p < .001$).

3. Results

3.1. Autophagic inducer results in whole blood parasitemia reduction and increase in survivability and parasite load within RPM

The increase in the F4/80 $^{+}$ CD68 $^{+}$ RPM population observed post inducer treatment (Fig. 1A and B). The F4/80 ^{low} CD68 $^{+}$ cells are not considered as RPM in our experiment as they have the partial admixed character of white pulp macrophages (F4/80 $^{-/low}$ CD68^{+}). Only the boxed cells marked as RPM in Fig. 1A were isolated with the gating strategy provided (Sup. Fig. 1A). RPM thus sorted from all the four treatment groups are checked for parasitemia load and also subjected for subsequent experiments. The parasite load in the whole blood decreased post autophagic inducer treatment, as measured by Giemsa Staining of the whole blood smear (Fig. 1C). However, the plasmodium load within the RPM increased in the same scenario of autophagic induction. This is measured by the percentage of cells showing positivity for merozoite surface protein 1 (Fig. 1C). The same result is observed when the plasmodium load in RPM subset, under different dose conditions, are also measured by amplifying the plasmodium 18 s rRNA from the cDNA prepared for real-time analysis (Fig. 1D). The mice set treated with rapamycin dose shows an effective increase in survivability as compared to the infected or autophagy inhibitor-treated (Fig. 1E).

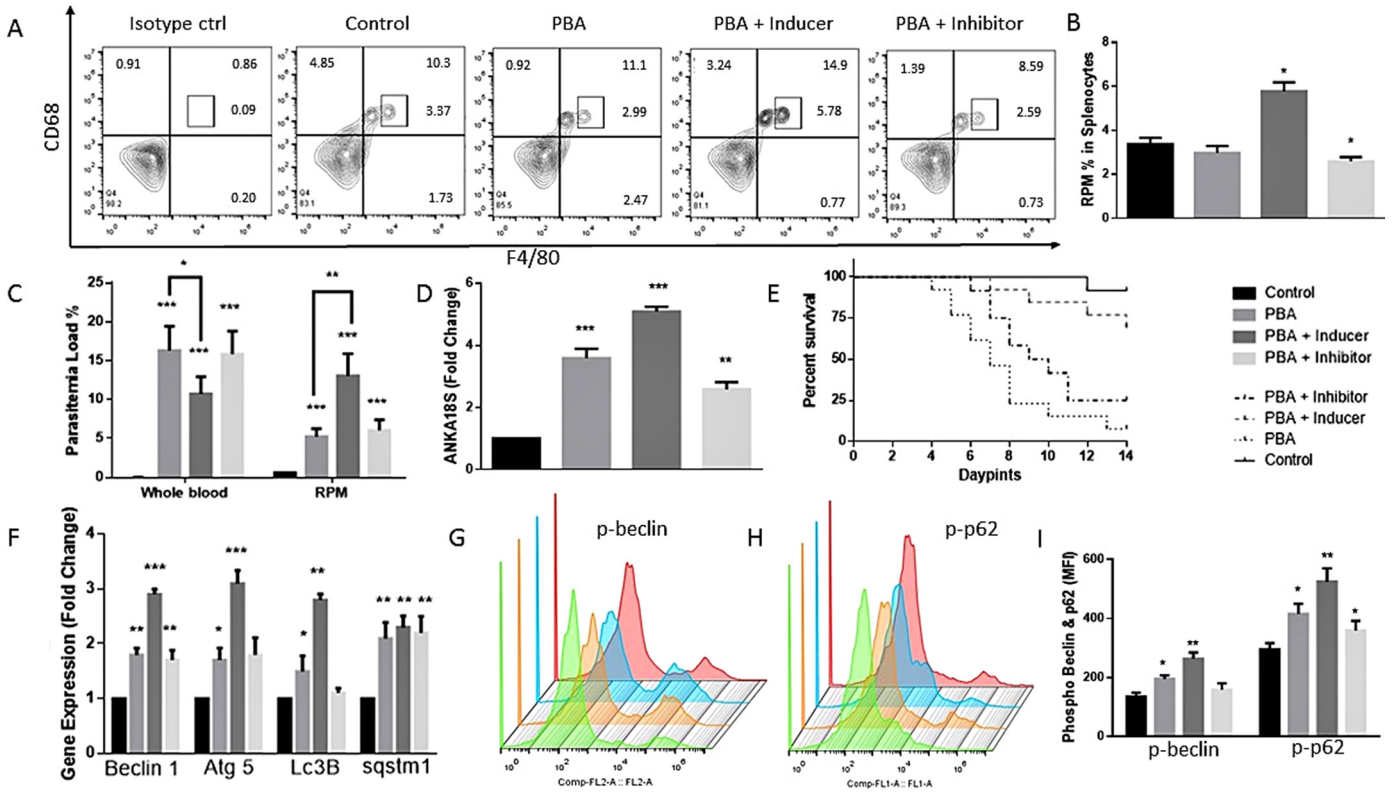

Fig. 1. Autophagic Gene expression of sorted RPM correlates with parasite clearance and survivability: A) RPM population as gated for F4/80^{+} CD68^{+} cells within the splenocytes increased post inducer treatment. The F4/80^{low} CD68^{+} cells are not considered as RPM in our experiment as they have the partial admixed character of white pulp macrophages (F4/80$^{-/low}$ CD68^{+}). Only the insert box-gate population marked as RPM is considered in all our experiments. The data shown here was acquired on 5×10^3 splenocytes. B) The significant increase in RPM in only PBA infected and more so in PBA + Inducer treated mice is observed C) The infected RBC percentage as measured by Giemsa staining and infected RPM percentage as measured by the cells positive for merozoite surface protein 1 (MSP1) by flow-cytometry staining. An increase in parasite load in autophagy induced RPM while whole blood parasite load drops D) Increased load of real-time ANKA18s expression post autophagic induction measured by isolating the whole RNA from RPM and reverse transcribed to cDNA and E) Increase in survivability post inducer treatment is observed as compared to other groups as analyzed by Kaplan-Meir survival analysis for 14 days on set of 12 mice per group. The analysis is provided in the Supplementary result section F) cDNA prepared from the RNA isolated from sorted out RPM from different treatment groups are checked for the gene expression status of the autophagic pathway which confirms an upregulation in the major autophagic genes. Isolated RPM is permeabilized with appropriate buffer and then incubated with the required antibody to detect the phosphorylation status of G) beclin S15 and H) p62 s403 where both are found to be I) significantly upregulated in the RPM isolated from mice set that received rapamycin inducer.
Data in graphs are the representative images derived from at least four independent experiments. Each round of experiments have five mice in each of the four sets: Control, PBA infected, PBA + Inducer, PBA + Inhibitor (*p < .05, **p < .01 and ***p < .001).

The autophagy marker genes like that of beclin, atg5 also increase post induction. This increment is greater than all other three sets as detected in quantitative real-time PCR (Fig. 1F). Autophagic induction is also evident from the marked enhancement in the phosphorylation level of beclin serine15 (Fig. 1G and I) and sqstm1 serine403 (Fig. 1H and I) residues post autophagic inducer treatment.

3.2. Rapamycin-treated mice shows enhancement in autophagosome formation and vacuolar LC3B deposition

The autophagic inducer treatment results in the upregulation of double positive cells with both parasitic protein MSP1 expression and autophagolysosome formation (Fig. 2A, Sup. Fig. 1B). We observed a drop in the initial autophagolysosome level in untreated infected RPM as compared to the control RPM. However, inducer treatment causes an increase in autophagolysosome level as well as the MSP1 level within the RPM (Fig. 2B). A positively proportionate increase in the antigen processing internal cellular marker of CD205 with that of vacuolar LC3B deposition is detected after washing off the free cytoplasmic LC3B (Fig. 2C and D).

3.3. LAMP1 expression, the phagocytic property of the RPM is enhanced post inducer treatment along with an insignificant change in adhesion property

We observed an increase in phagocytosis rate of fluorochrome tagged zymosan granules by the RPM sorted from the infected spleen treated with autophagic inducer (Fig. 3A and C, Sup. Fig. 1C).

However, the adhesion property of RPMs are checked by calceinAM labeled control RBC (cRBC) or infected RBC (iRBC). The labeled cells from the respective mice set are superimposed on sorted RPM subset in optimum culture condition. The percentage of calcein AM signal detected indicates an insignificant change in adhesion property of the autophagy induced RPMs as compared to the control or infected set (Fig. 3B and C, Sup Fig. 1C).

We checked the expression level of Lysosomal-associated membrane protein (LAMP- I and LAMP II) within the sorted RPM. CD107a and CD107b are the exclusive markers for the two LAMP proteins present within the macrophages. The sorted RPM stained with these two marker antibodies shows an increase double positive cell population (Fig. 3D and E). This confirms the increase in associated lysosomal activity post rapamycin treatment.

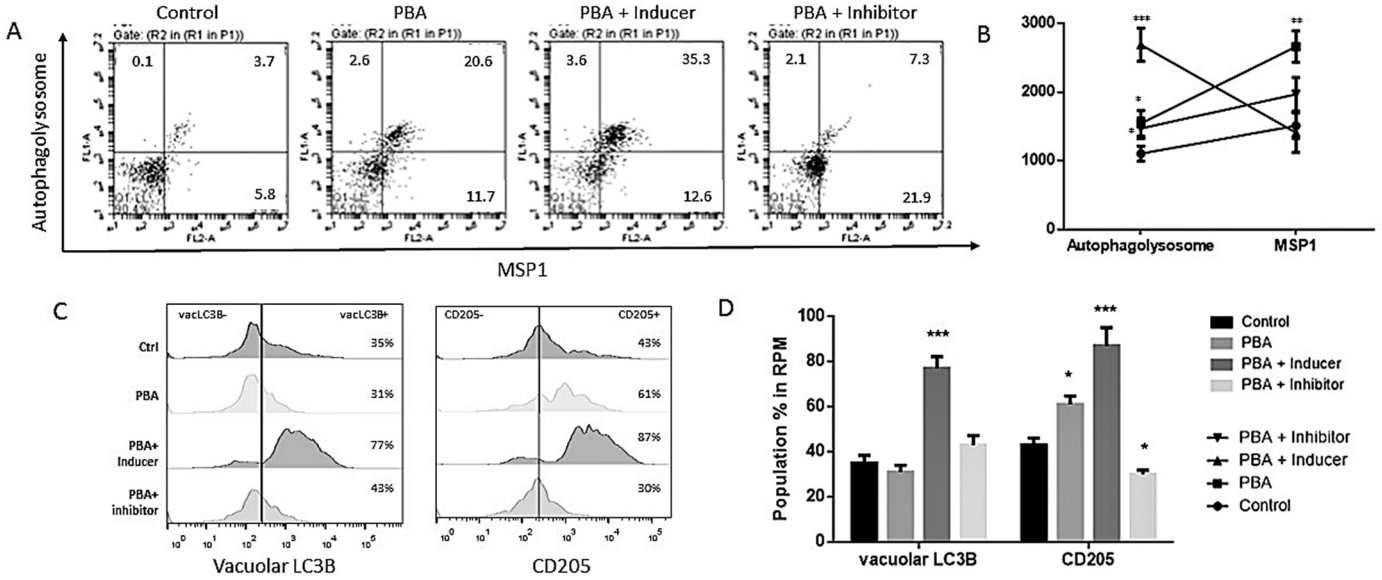

Fig. 2. Autophagolysosome - MSP1 expressing double positive cells increased post autophagic induction accompanied with enhanced deposition of vacuole bound LC3B and CD205 expression: A) Isolated RPM is stained with the autophagolysosome detection dye and MSP1 protein and we found an increase in double positive cells having both the autophagolysosome formation and parasite load increase post inducer treatment B) When plotted the mean fluorescence intensity measured from the last experiment it shows a drop in autophagolysosome formation in infected RPM as compared to control RPM, which again got enhanced post inducer treatment along with the high MSP1 load entrapped within those cells. Flowcellect kit procedure followed where the cytoplasmic LC3B within RPM is washed out, leaving only the vacuole bound autophagy pathway involved LC3B; and C) we find an enhanced RPM population having vacuolar LC3B deposition while autophagy is induced, D) which is positively correlated with RPM population possessing the antigen processing marker protein CD205. E) The positive cell population is plotted in bar diagram shows a significant increase in LC3B and CD205 post autophagic induction.
Data in graphs are the representative images derived from at least four independent experiments. Each round of experiments have five mice in each of the four sets: Control, PBA infected, PBA + Inducer, PBA + Inhibitor (*p < .05, **p < .01 and ***p < .001).

3.4. Co-stimulatory markers, MHC molecule expression, Antigen presentation marker of RPMs enhanced post autophagic induction thus skewing RPM subset to M1 subtype

Isolated RPM are co-stained with M2 subtype marker antibodies CD163 and CD206, both having the same fluorochrome conjugate. The difference in population percentage for M2 subtype of RPM subset thus observed clearly shows a significant drop of the same post inducer treatment (Fig. 4A and B. Sup Fig. 1F). Thus, unstained M1 subtype of the RPM subset increase in the same treatment condition (Fig. 4A and B). The same is confirmed by staining the isolated RPM with M1 subtype marker antibodies iNOS and TLR2 (Sup. Fig. 2A, 2B). The staining of any individual antibody differentiate M1 from M2 polarized macrophage. We used two for each subtype case. MHCI and MHCII expressing RPM population increased both in M1 and M2 subtypes (Fig. 4C and D). The increase is more pronounced in M1 subtype. However the CD80- CD86 expressing double positive RPM population enhanced post inducer treatment in M1 subtype but not so in M2 subtype (Fig. 4D and E).

3.5. Increase in splenic infiltration of neutrophil and CD4 + T cells due to enhanced chemokine-mediated recruitment signal by autophagy induced RPM

An increase in neutrophil ($CD11b^+$ $Ly6G^+$) (Fig. 5A and C) and CD4T ($CD4^+$) (Fig. 5B and C) within the isolated splenocytes from the whole spleen is observed post induction of autophagic flux.

Our data figures out an inverse relationship in the dropped expression of nf-kb inhibitor A20, with that of the increased level of both CXCL1 and CXCL2 post autophagic induction (Fig. 5D, Sup. Fig. 3A, B, C). Both of these chemokines were reported to facilitate neutrophil infiltration process towards red pulp zone.

The isolated RPM secretes more of chemokines CXCL9, CXCL11, and CXCL13 when it is under the autophagic induced condition and co-incubated with iRBC in cell culture setup (Fig. 5E and F). These chemokine ligands have their respective receptors of CXCR3 (for CXCL9 and CXCL11) and CXCR5 (for CXCL13) on CD4T cells. The upregulation of both CXCR3 and CXCR5 on helper CD4T cells indicate that chemokine secretion by RPM plays a key role in facilitating the infiltration of CD4T cells and its recruitment in red pulp zone (Fig. 5G and H).

4. Discussion

Rapamycin has previously been used in a number of studies in the ECM model and is reported to play a beneficial role for the host with a significant increase in survivability [3,27,37]. Different dose regimen has been followed in previous works with variation, both in terms of concentration and number of doses [3,27,37]. While a group suggests this dose to be administered within first 4 days of infection [3], other group shows that even a single dose at the late stage of the disease is enough for better disease outcome [27]. Gordon et al. show a rapamycin treatment in conjunction with artesunate treatment results in a significant increase in survival of *Pb*A-infected mice [3]. This study traces the role of splenic red pulp macrophages in ECM, after rapamycin-mediated induction of autophagic flux.

Autophagy induction causes an increase of $F4/80^+CD68^+$ splenic RPM subsets (Fig. 1A). Establishing our autophagic modulation model, we checked the alteration in autophagic gene expression status via quantitative real-time PCR (Fig. 1F) and measured the phosphorylation of the beclin serine15 and sqstm1 serine403 (Fig. 1G, H and I). Increased phosphorylation of those two serine residues in the respective proteins is the already known marker for autophagic induction [38,39]. We found a clear beneficial change in the survivability post autophagic inducer treatment (Fig. 1E), with better parasite clearance from the whole blood (Fig. 1C) and enhanced entrapping of the same by RPM (Fig. 1C and D). Although previous reports suggest that the peripheral or whole blood parasitemia be increased post rapamycin treatment [3,27,37], we find a significant reduction of the same. This might be

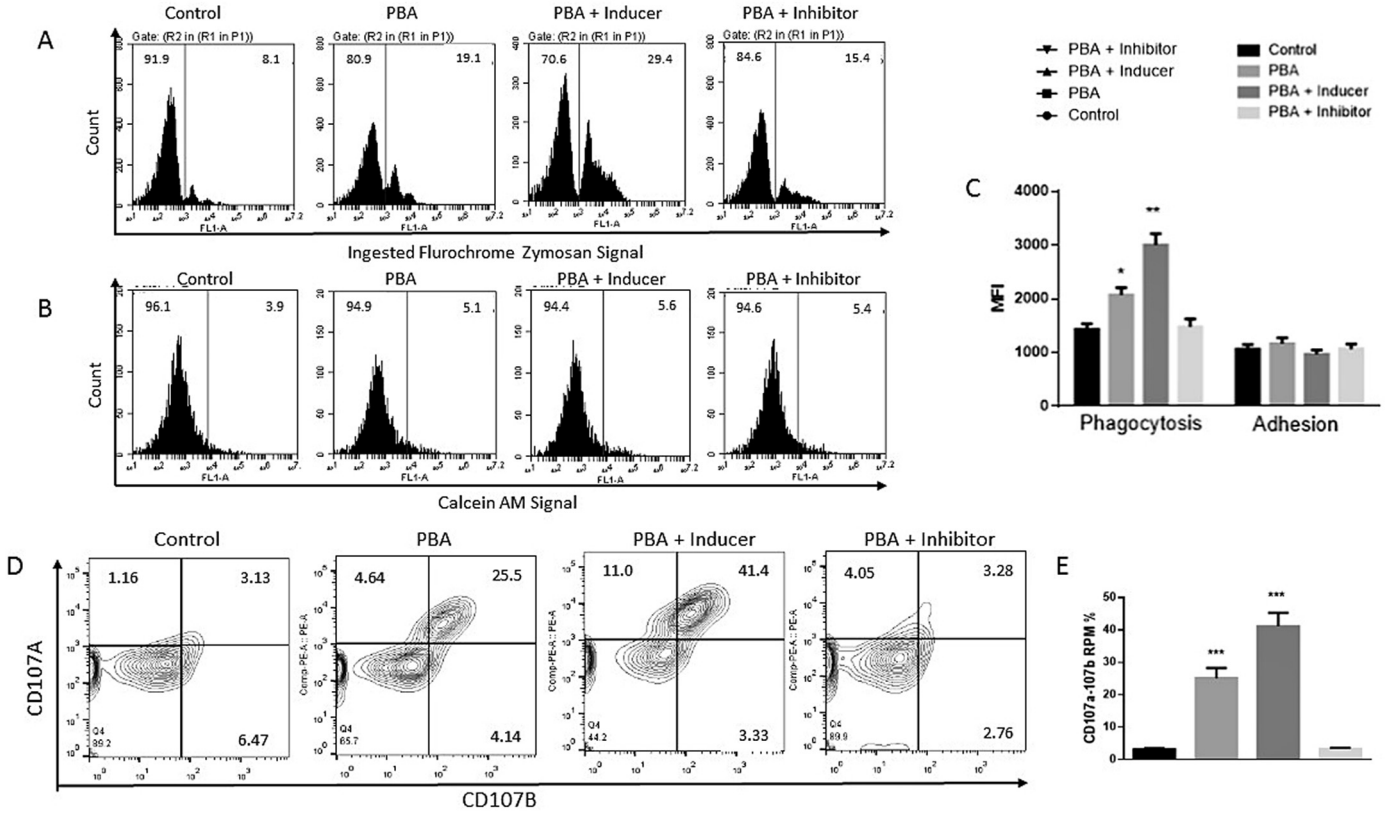

Fig. 3. Increase in phagocytic potential without any significant alteration in adhesion property observed along with an increase in RPM population exhibiting increased LAMP I and II expression post inducer treatment: A) Increase in the isolated RPM cell population ingesting the zymosan granules in the in-vitro phagocytosis assay are observed in autophagy induced condition. The RPM isolated are incubated with the zymosan A fluorochrome granules and co-incubated with the control RBC (cRBC) or infected RBC (iRBC). The histogram is showing the cell populations percentage in different treatment groups where we find a considerable increase in cell population ingesting the zymosan granules post autophagy induction. B) Calcein AM-labeled cRBC, or iRBC collected are coincubated with the isolated RPM in cell culture setup to study the adhesion property of the cells. The RPM population showing adhesion property remains relatively unchanged in all treatment groups C) The mean fluorescence intensity signal increased during detection of phagocytosis property and not during the detection of adhesion property by the cells; as the later remains unaltered post induction. D) Isolated RPM shows an increase in Lysosomal Associated Membrane protein (LAMP I and LAMP II) expression with the autophagy induction. CD107A (for LAMP I) and CD107B (for LAMP II) are co-stained and E) double positive cell population is plotted in a bar diagram, which shows a significant increase of the same in both the PBA infected and PBA+ inducer treated condition.
Data in graphs are the representative images derived from at least four independent experiments. Each round of experiments have five mice in each of the four sets: Control, PBA infected, PBA + Inducer, PBA + Inhibitor (*p < .05, **p < .01 and ***p < .001).

due to different factors like higher dose concentration used by us, and also the number of doses, doses starting even before the parasite is introduced, and Swiss albino mice model that we have used for the experiments. The cumulative effect of these factors results in better autophagic induction which might be a promoting factor for better parasite clearance.

While checking the autophagolysosome formation by staining with the catiophillic amphitacer dye, we find an increase in the same while autophagy is induced (Fig. 2A and B). Increase in the RPM cell population possessing both the pathogens and autophagolysosome is observed (Fig. 2A and B). The plasmodium load is detected by the presence of the merozoite surface marker protein. This proves the efficient autophagic induction with the parasite-laden cells post inducer treatment. Enhancement in the autophagic vacuole bound LC3B protein is noticed in set C after cytoplasmic free LC3B is washed off (Fig. 2C and E). This, yet again, proves a positive autophagic induction post inducer treatment. A positive correlation is observed in the expression of vacuolar LC3B with that of a novel endocytic receptor CD205 that is reported to mediate antigen uptake and presentation and cross-presentation to T cells (Fig. 2D and E). Hence, we conclude that rapamycin treatment induces autophagolysosome formation and autophagic vacuole bound LC3B deposition along with enhanced CD205 expression in parasite-laden RPM.

While checking the adhesive property of the RPM, we do not find any significant change in its attachment with the calcein-labeled iRBC (Fig. 3B and C). However, an enhanced phagocytic property in the autophagy induced RPMs is observed (Fig. 3A and C). It indicates that autophagy flux positively regulates the engulfing of the pathogens without overburdening the cells by adhering them with an increased pathogenic load on their surface. Accumulation of increased autophagic vacuoles can also be observed in scenarios where lysosome number and function is reduced [40]. Lysosomal-associated membrane protein I and II (LAMP I and LAMP II) forms almost 50% of lysosomal surface protein. Their increase with the autophagolysosome formation confirms the active ongoing autophagic pathway within the RPM post inducer treatment (Fig. 3D and E).

Autophagy induced polarization of RPM subset towards M1 subtype is observed (Fig. 4A and B). While studying the RPM activity in terms of their antigen presentation and co-stimulation of immune response, we find a significantly MHCI and MHCII in both M1 and M2 subtypes of RPM (Fig. 4C and D). Being more aggressive M1 subtype shows more pronounced MHC expression pattern as well as increased CD80-CD86 double positive population than M2 subtype (Fig. 4C and E), post inducer treatment. A shift from M2 to M1 macrophage subtype demonstrates an active and aggressive immune function performed by RPM subset [41].

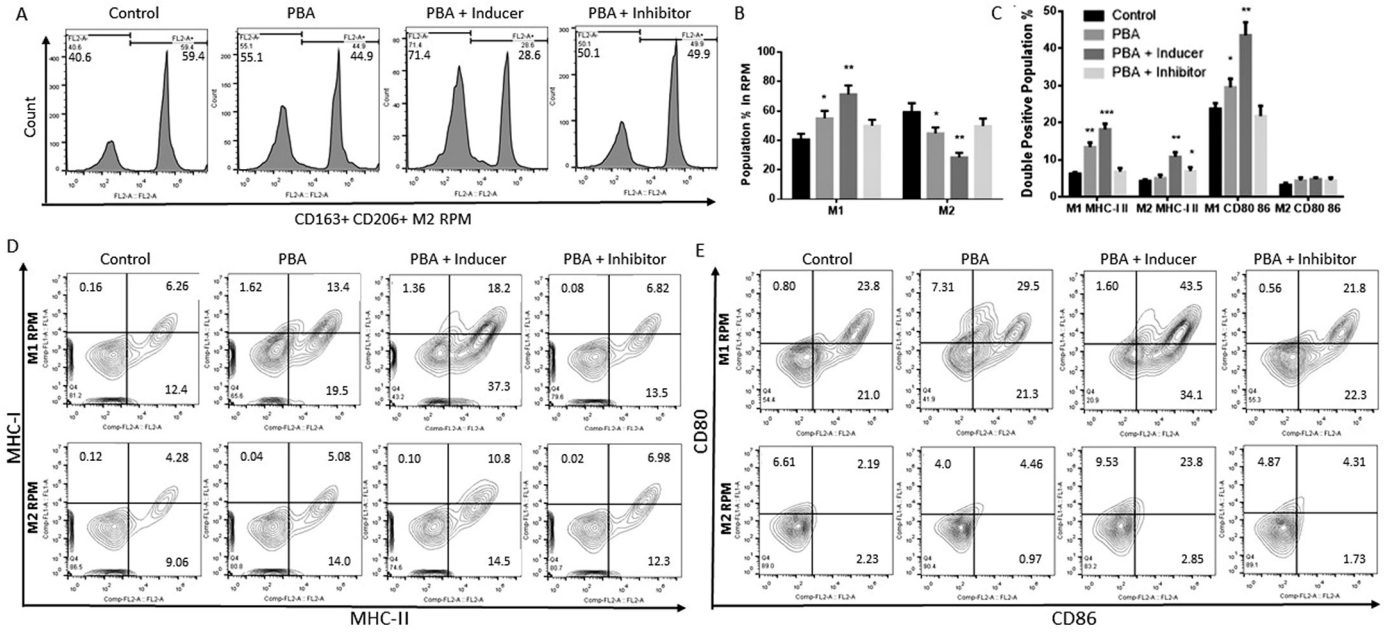

Fig. 4. Costimulatory molecule CD80 CD86 expression, major histocompatibility complex I and II synthesis increased post autophagic induction resulting in skewing of RPM subset to M1 subtype: A) The skewing of the RPM population towards M1 polarization with a drop in the M2 subtype RPM post inducer treatment is observed. The isolated RPM is stained with CD163-PE and CD206-PE, the markers of M2 macrophage subtype. The RPM thus obtained in Filter 2 (for PE) is of M2 subtype, and unstained cells are M1 subtype. M1 subtyping is further confirmed (Sup. Fig. 2A, 2B) where iNOS-PE and TLR2-PE antibodies are used to get stained M1 population. B) The bar diagram plotting shows a significant increase in M1 subtype with the corresponding drop in M2 polarized RPM population post autophagic induction. C, D) The increase in MHCI and MHCII double positive M1 polarized RPM population (D, upper panel) and M2 polarized RPM population (D, lower panel) is observed post autophagic induction. C, E) However RPM population showing double positive for costimulatory marker CD80 and CD86 is higher in autophagy induced M1 polarized RPM (E, upper panel) and not so in M2 polarized RPM (E, lower panel).
Data in graphs are the representative images derived from at least four independent experiments. Each plot of flow-cytometry results shown was done on 5×10^3 cells. Each round of experiments have five mice in each of the four sets: Control, PBA infected, PBA + Inducer, PBA + Inhibitor (*$p < .05$, **$p < .01$ and ***$p < .001$).

Interestingly two major cytokines influencing macrophage function and activity are IL10 and IL 12. The cytokine levels are measured by ELISA on the cell culture supernatants of each of the isolated RPM from different treatment groups. Interestingly, the drop in anti-inflammatory IL10 level along with a considerable increase in IL12 level is observed (Sup Fig. 3D). Previous reports show IL10 causes suppression of the anti-pathogenic activity of macrophages [42]. On the other hand, IL12 causes M1 macrophage polarization with efficient pathogenic clearance and costimulatory marker expression [43].

Autophagy induced increase in the population of neutrophil (Fig. 5A and C) and CD4T cells (Fig. 5B and C) in the spleen as measured by flow cytometry staining might play a crucial role in eliciting immune response necessary for combatting against the infection. However, the signaling cue for recruitment or infiltration of these two cell types can be traced by the chemokine secretion by RPM and their corresponding receptor expression pattern on the respective cells.

Previous reports show autophagy-mediated degradation of the NF-kB inhibitor molecule A20 [16] causes the release of CXCL1 and CXCL2 resulting in the neutrophil recruitment in spleen by RPM [16]. Autophagic induction in infected RPM results in a drop of A20 level in set C resulting in the higher release of CXCL1 and CXCL2. This, according to the previous reports, [16] must facilitate in the neutrophil infiltration within the splenic red pulp zone (Fig. 5D, Sup. Fig:3A,3B,3C). Recruitment of neutrophil to the blood filtering splenic red pulp zone might be a crucial determinant for inducing better host immune response against Plasmodium. Further studies on the immune interaction of neutrophil, post RPM induced infiltration, may highlight their role in details.

RPM produces chemokines like CXCL9, CXCL11, and CXCL13 that directly bind with the CXCR3 and CXCR5 that are found to be upregulated in CD4 + T cells. This helps to initiate signaling essential for recruitment off helper T cells [44]. mTOR prevents antigen-stimulated CD4 and CD8 T cell homing and trafficking by redirecting them to the site of inflammation [22,45]. We found mTOR suppression with autophagic inducer rapamycin facilitates chemokine signaling mediated homing of CD4T cells to the spleen. CXCL9, CXCL11, and CXCL13 expression enhanced in RPM post inducer treatment (Fig. 5E and F).

Interestingly the respective receptors of these chemokine ligands are present on CD4T helper cells. The autophagy induced enhanced expression level of those receptors (CXCR3 and CXCR5) on CD4T cell signifies regulation in recruiting those cells in the splenic red pulp zone (Fig. 5G and H). Thus, we can infer autophagic enhancement positively influence the infiltration of both neutrophil and helper CD4T cells via chemokine regulation. However, further study on whether RPM can prime the T cells and modulate their action might be interesting in understanding their role in experimental cerebral malaria model.

Our study has its limitation due to the lack of any known potential autophagic inducer that can specifically affect the splenic RPM and not any other cells. Rapamycin used for autophagic induction must have a systemic effect on multiple other cell types causing it challenging to pinpoint RPM to be the 'sole' cause of better host response. Nevertheless, RPM exhibits a better immune response in autophagy induced set in all the experiments performed by us. Although, whether the response is the causal effect formed by RPM only or is the significant impact from the cumulative contribution from multiple cellular types is yet to decipher in future studies. More in-depth study at the molecular level will help us to decipher the mechanistic details underplaying 'enhanced autophagy within RPM' with 'better immune response against Plasmodium.' As of now, we can state the association between these two factors is evident from our study.

Previous reports suggest that another autophagy inducer molecule torins do clear off the malarial parasite with perfection [29].

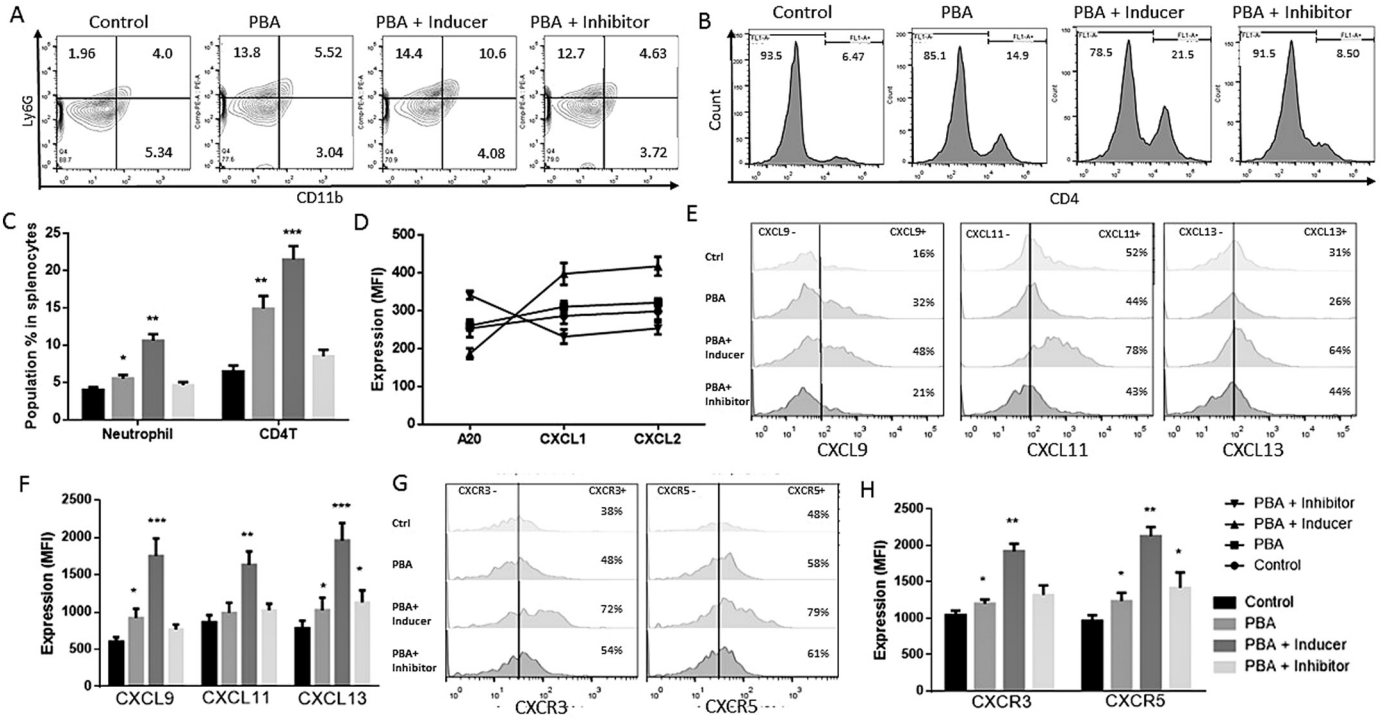

Fig. 5. Autophagy induced RPM shapes chemokine mediated infiltration signal for recruiting neutrophil and CD4T cells to red pulp zone of spleen: A) $CD11b^{+}Ly6G^{+}$ neutrophils population percentage within the splenocytes increased post inducer treatment as compared to other groups, B) CD4T cell population also do increase within the whole spleen as measured by $CD4^{+}$ staining C) The significant increase in the population percentage of neutrophils and CD4T cells is plotted in the bar diagram D) NF-kb pathway protein A20 level drop inversely correlates with CXCL1 and CXCL2 expression, signifying a positive induction for neutrophil recruitment. The data of the same is provided in Sup. Fig:3A,3B,3C with the statistical significance bar diagram plot E) Three panels shows the increase in the population percentage showing positive expression of CXCL9, CXCL11, and CXCL13 respectively, within isolated RPMs from post inducer treated mice set. F) Expression level of CXCL9, CXCL11, CXCL13 within the RPM isolated from different treatment groups are detected by flow cytometric method and mean fluorescence intensity is plotted G) CD4T cell population shows upregulation in surface receptors of CXCR3 (receptor for CXCL9, CXCL11) and CXCR5 (receptor for CXCL13) in two panels respectively post autophagic induction. H) The level of the CXCR3 and CXCR5 are measured by flow cytometry methods, and their mean fluorescence intensity is plotted.

Data in graphs are the representative images derived from at least four independent experiments. Each round of experiments have five mice in each of the four sets: Control, PBA infected, PBA + Inducer, PBA + Inhibitor (*p < .05, **p < .01 and ***p < .001). (For interpretation of the references to colour in this figure legend, the reader is referred to the web version of this article.)

Autophagic induction does help in pathogenic degradation in a large number of diseases. Over here, we have shown a better host immune response affecting enhanced parasite clearance and survivability post autophagic induction. As red pulp macrophages play a crucial role in the immune processing of the infected RBC flowing through them, a drug targeted towards them to induce the autophagic flux might be beneficial for the host to have a better treatment during Plasmodium infection.

Author's contribution

Anirban Sengupta designs and carries out the main project and experiments; supported by Saikat Mukherjee and Soubhik Ghosh. Tarun Keswani and Samrat Sarkar helped in preparing the manuscript and also in parts of data analysis and interpretation. Arindam Bhattacharyya guides the project workflow from the beginning.

Conflict of interest

Authors declare that there is no conflict of interest in publishing this article.

Acknowledgments

Department of Science and Technology, India (SB/SO/HS-106/2013, dated 21/11/2014), Department of Atomic Energy, Board of Research in Nuclear Sciences (DAE -BRNS), India: (37(1)/14/54/2014-BRNS/1740 dated 28.10.2014), West Bengal Department of Biotechnology, India (22(Sanc)/BT (Estt)/RD-20/2013 dated 07/01/2015).

Calcutta University- BD Centre of Excellence Flow Cytometry Facility [CU-BD CoE (CRNN)] for cell sorting and flow cytometry.

Special thanks to Sunipa Roy, MA English, faculty at Him International School for checking and modifying the manuscript writeup.

Appendix A. Supplementary data

Supplementary data to this article can be found online at https://doi.org/10.1016/j.parint.2019.03.008.

References

[1] L. Rénia, S.W. Howland, C. Claser, A. Gruner, R. Suwanarusk, T. Teo, B. Russell, L.F. Ng, Cerebral malaria: mysteries at the blood-brain barrier, Virulence 3 (2012) 193–201, https://doi.org/10.4161/viru.19013.

[2] A.G. Craig, G.E. Grau, C. Janse, J.W. Kazura, D. Milner, J.W. Barnwell, G. Turner, J. Langhorne, Participants of the Hinxton Retreat meeting on Animal Models for Research on Severe Malaria, The role of animal models for research on severe malaria, PLoS Pathog. 8 (2012) e1002401, , https://doi.org/10.1371/journal.ppat.1002401.

[3] E.B. Gordon, G.T. Hart, T.M. Tran, M. Waisberg, M. Akkaya, J. Skinner, S. Zinöcker, M. Pena, T. Yazew, C.-F. Qi, L.H. Miller, S.K. Pierce, Inhibiting the mammalian target of rapamycin blocks the development of experimental cerebral malaria, mBio 6 (3) (2015) e00715–e00725, https://doi.org/10.1128/mBio.00725-15.

[4] L. Schofeld, G.E. Grau, Immunological processes in malaria pathogenesis, Nat. Rev. Immunol. 5 (2005) 722–735.

[5] J.A. McQuillan, A.J. Mitchell, Y.F. Ho, V. Combes, H.J. Ball, J. Golenser, et al., Coincident parasite and CD8 T cell sequestration is required for development of experimental cerebral malaria, Int. J. Parasitol. 41 (2011) 155–163.

[6] A. Haque, S.E. Best, K. Unosson, F.H. Amante, F. de Labastida, N.M. Anstey, et al., Granzyme B expression by CD8+ T cells is required for the development of experimental cerebral malaria, J. Immunol. 186 (2011) 6148–6156.

[7] B. Schnitzer, T. Sodeman, M.L. Mead, P.G. Contacos, Pitting function of the spleen in malaria: ultrastructural observations, Science 177 (1972) 175–177, https://doi.org/10.1126/science.177.4044.175.

[8] S. Leoni, D. Buonfrate, A. Angheben, F. Gobbi, Bisoffi Z the hyper-reactive malarial splenomegaly: a systematic review of the literature, Malar. J. 14 (2015 Apr 29) 185, https://doi.org/10.1186/s12936-015-0694-3 Review. (25925423).

[9] V. Deretic, T. Saitoh, S. Akira, Autophagy in infection, inflammation and immunity, Nat. Rev. Immunol. 13 (10) (2013 Oct) 722–737, https://doi.org/10.1038/nri3532 (Review).

[10] Z. Chen, T. Wang, Z. Liu, G. Zhang, J. Wang, S. Feng, J. Liang, Inhibition of autophagy by MiR-30A induced by mycobacteria tuberculosis as a possible mechanism of immune escape in human macrophages, Jpn. J. Infect. Dis. 68 (5) (2015) 420–424, https://doi.org/10.7883/yoken.JJID.2014.466 (Epub 2015 Apr 10).

[11] D.J. Puleston, A.K. Simon, Autophagy in the immune system, Immunology 141 (1) (2014 Jan) 1–8, https://doi.org/10.1111/imm.12165 (Review).

[12] R.S. Flannagan, V. Jaumouillé, S. Grinstein, The cell biology of phagocytosis, Annu. Rev. Pathol. 7 (2012) 61–98, https://doi.org/10.1146/annurev-pathol-011811-132445 (Epub 2011 Sep 9. Review).

[13] T. Keswani, A. Bhattacharyya, Splenocyte apoptosis in Plasmodium berghei ANKA infection: possible role of TNF-α and TGF-β, Parasite Immunol. 35 (2) (2013 Feb) 73–90, https://doi.org/10.1111/pim.12005.

[14] S.J. Higgins, K. Xing, H. Kim, D.C. Kain, F. Wang, A. Dhabangi, et al., Systemic release of high mobility group box 1 (HMGB1) protein is associated with severe and fatal Plasmodium falciparum malaria, Malar. J. 12 (2013) 105, https://doi.org/10.1186/1475-2875-12-105.

[15] H. Borges da Silva, R. Fonseca, R.M. Pereira, A.A. Cassado, J.M. Álvarez, M.R. D'Império Lima, Splenic macrophage subsets and their function during bloodborne infections, Front. Immunol. 6 (2015) 480, https://doi.org/10.3389/fmmu.2015.00480.

[16] M. Kanayama, M. Inoue, K. Danzaki, G. Hammer, Y.W. He, M.L. Shinohara, Autophagy enhances NFκB activity in specifc tissue macrophages by sequestering A20 to boost antifungal immunity, Nat. Commun. 6 (2015) 5779, , https://doi.org/10.1038/ncomms6779.

[17] K. De Filippo, A. Dudeck, M. Hasenberg, E. Nye, N. van Rooijen, K. Hartmann, M. Gunzer, A. Roers, N. Hogg, Mast cell and macrophage chemokines CXCL1/CXCL2 control the early stage of neutrophilrecruitment during tissue inflammation, Blood 121 (24) (2013 Jun 13) 4930–4937, https://doi.org/10.1182/blood-2013-02-486217. Epub 2013 May 3.

[18] E. Gwyer Findlay, A. Villegas-Mendez, J.B. de Souza, C.A. Inkson, T.N. Shaw, C.J. Saris, et al., IL-27 receptor signaling regulates CD4+ T cell chemotactic responses during infection, J. Immunol. 190 (2013) 4553–4561, https://doi.org/10.4049/ jimmunol.1202916.

[19] D. Kurotaki, T. Uede, T. Tamura, Functions and development of red pulp macrophages, Microbiol. Immunol. 59 (2) (2015 Feb) 55–62, https://doi.org/10.1111/1348-0421.12228 (Review).

[20] M. Naito, S.I. Hayashi, H. Yoshida, K. Takahashi, Abnormal differentiation of tissue macrophage populations in “osteopetrosis” (op) mice defective in the production of macrophage colony-stimulating factor (M-CSF) or CSF-1, Am. J. Pathol. 139 (1991) 657–667.

[21] D. Kurotaki, S. Kon, K. Bae, K. Ito, Y. Matsui, Y. Nakayama, et al., CSF-1-dependent red pulp macrophages regulate CD4 T cell responses, J. Immunol. 186 (2011) 2229–2237, https://doi.org/10.4049/jimmunol.1001345.

[22] C. Liu, N.M. Chapman, P.W. Karmaus, H. Zeng, H. Chi, mTOR and metabolic regulation of conventional and regulatory T cells, J. Leukoc. Biol. 97 (2015) 837–847.

[23] T. Weichhart, M. Hengstschlager, M. Linke, Regulation of innate immune cell function by mTOR, Nat. Rev. Immunol. 15 (2015) 599–614.

[24] L. Veletzky, K. Rehman, T. Lingscheid, W. Poeppl, F. Loetsch, H. Burgmann, et al., In vitro activity of immunosuppressive drugs against Plasmodium falciparum, Malar. J. 13 (2014) 476.

[25] N. Bharatham, M.W. Chang, H.S. Yoon, Targeting FK506 binding proteins to fight malarial and bacterial infections: current advances and future perspectives, Curr. Med. Chem. 18 (2011) 1874–1889, https://doi.org/10.2174/092986711795496818.

[26] Y. Odaka, B. Xu, Y. Luo, T. Shen, C. Shang, Y. Wu, et al., Dihydroartemisinin inhibits the mammalian target of rapamycin-mediated signaling path- ways in tumor cells, Carcinogenesis 35 (2014) 192–200.

[27] Y.G. Zhao, Y. Wang, Z. Guo, A.D. Gu, H.C. Dan, A.S. Baldwin, et al., Dihydroartemisinin ameliorates inflammatory disease by its reciprocal efects on Th and regulatory T cell function via modulating the mammalian target of rapamycin pathway, J. Immunol. 189 (2012) 4417–4425.

[28] P. Mejia, J.H. Trevino-Villarreal, C. Hine, E. Harputlugil, S. Lang, E. Calay, et al., Dietary restriction protects against experimental cerebral malaria via leptin modulation and T-cell mTORC1 suppression, Nat. Commun. 6 (2015) 6050.

[29] K.K. Hanson, A.S. Ressurreição, K. Buchholz, M. Prudêncio, J.D. HermanOrnelas, M. Rebelo, W.L. Beatty, D.F. Wirth, T. Hänscheid, R. Moreira, M. Marti, M.M. Mota, Torins are potent antimalarials that block replenishment of Plasmodium liver stage parasitophorous vacuole membrane proteins, Proc. Natl. Acad. Sci. U. S. A. 110 (2013) E2838–E2847, https://doi.org/10.1073/pnas.1306097110.

[30] W. Sun, T.Q. Tanaka, C.T. Magle, W. Huang, N. Southall, R. Huang, et al., Chemical signatures and new drug targets for gametocytocidal drug development, Sci. Rep. 4 (2014) 3743.

[31] Noboru Mizushima, Tamotsu Yoshimorim, Beth Levine, Methods in mammalian research, Cell 140 (3) (2010 Feb 5) 313–326, https://doi.org/10.1016/j.cell.2010.01.028.

[32] S.J. Seguin, F.F. Morelli, J. Vinet, D. Amore, S. De Biasi, A. Poletti, D.C. ubinsztein, S. Carra, Inhibition of autophagy, lysosome and VCP function impairs stress granule assembly, Cell Death Differ. 21 (2014) 1838–1851.

[33] Sun R[1], Y. Luo, J. Li, Q. Wang, J. Li, X. Chen, K. Guan, Z. Yu, Ammonium chloride inhibits autophagy of hepatocellular carcinoma cells through SMAD2 signaling, Tumour Biol. 36 (2) (2015 Feb) 1173–1177, https://doi.org/10.1007/s13277-014-2699-x. Epub (2014 Oct 24).

[34] L.L. Chan, D. Shen, A.R. Wilkinson, W. Patton, N. Lai, E. Chan, D. Kuksin, B. Lin, J. Qiu, A novel image-based cytometry method for autophagy detection in living cells, Autophagy 8 (9) (2012 Sep) 1371–1382, https://doi.org/10.4161/auto.2102822895056.

[35] W.P. Huang, T. Shintani, Z. Xie, Assays for autophagy I: the Cvt pathway and nonselective autophagy, Methods Mol. Biol. 1163 (2014) 153–164 PMID: 24841304 https://doi.org/10.1007/978-1-4939-0799-1_10.

[36] S. Yamasaki, M. Matsumoto, O. Takeuchi, T. Matsuzawa, E. Ishikawa, M. Sakuma, H. Tateno, J. Uno, J. Hirabayashi, Y. Mikami, K. Takeda, S. Akira, T. Saito, C-type lectin Mincle is an activating receptor for pathogenic fungus, Malassezia, Proc. Natl. Acad. Sci. U. S. A. 106 (6) (2009 Feb 10) 1897–1902, https://doi.org/10.1073/pnas.0805177106 (Epub 2009 Jan 26).

[37] Y.H. Lee, O. Shynlova, S.J. Lye, Stretch-induced human myometrial cytokines enhance immune cell recruitment via endothelialactivation, Cell Mol. Immunol. 12 (2) (2015 Mar) 231–242, https://doi.org/10.1038/cmi.2014.39 (Epub 2014 Jun 2).

[38] Sheila Donnelly, Wilhelmina M. Huston, Michael Johnson, Natalia Tiberti, Bernadette Saunders, Bronwyn O'Brien, Catherine Burke, Maurizio Labbate, Valery Combes, Targeting the master regulator mTOR: a new approach to prevent the neurological of consequences of parasitic infections? Parasit. Vectors 10 (2017) 581, https://doi.org/10.1186/s13071-017-2528-3.

[39] Y. Wei, Z. An, Z. Zou, R. Sumpter, M. Su, X. Zang, S. Sinha, M. Gaestel, B. Levine, The stress-responsive kinases MAPKAPK2/MAPKAPK3 activate starvation-induced autophagy through Beclin 1 phosphorylation, Elife 4 (2015 Feb 18), https://doi.org/10.7554/eLife.05289.

[40] G. Matsumoto, K. Wada, M. Okuno, M. Kurosawa, N. Nukina, Serine 403 phosphorylation of p62/SQSTM1 regulates selective autophagic clearance of ubiquitinated proteins, Mol. Cell 44 (2) (2011 Oct 21) 279–289, https://doi.org/10.1016/j.molcel.2011.07.039.

[41] R.W. Button, S.L. Roberts, T.L. Willis, C.O. Hanemann, S. Luo, Accumulation of autophagosomes confers cytotoxicity, J. Biol. Chem. 292 (33) (2017 Aug 18) 13599–13614, https://doi.org/10.1074/jbc.M117.782276 (Epub 2017 Jul 3).

[42] Klaus Ley, M1 means kill; M2 means heal, J. Immunol. 199 (7) (October 1, 2017) 2191–2193, https://doi.org/10.4049/jimmunol.1701135.

[43] M. Niikura, S. Inoue, F. Kobayashi, Role of Interleukin-10 in malaria: focusing on Coinfection with lethal and nonlethal murine malaria parasites, J Biomed Biotechnol 2011 (2011) 383962, , https://doi.org/10.1155/2011/383962 (Epub 2011 Nov 13).

[44] X. Ma, W. Yan, H. Zheng, Q. Du, L. Zhang, Y. Ban, N. Li, F. Wei, Regulation of IL-10 and IL-12 production and function in macrophages and dendritic cells.,F1000Res, 4 (2015 Dec 17), https://doi.org/10.12688/f1000research.7010.1 pii: F1000 Faculty Rev-1465. (eCollection 2015).

[45] N. Karin, G. Wildbaum, The role of chemokines in shaping the balance between CD4(+) T cell subsets and its therapeutic implications in autoimmune and Cancer diseases, Front. Immunol. 6 (2015 Nov 30) 609, https://doi.org/10.3389/fimmu.2015.00609. eCollection 2015.